Arabian Journal for Science and Engineering
https://doi.org/10.1007/s13369-023-08584-0

RESEARCH ARTICLE-MECHANICAL ENGINEERING

Experimental Investigation, Modeling and Optimization of Parameters in Hard Anodizing of 6063 Aluminum Alloy Using Central Composite Design

Vahid Pouyafar[1] · **Ramin Meshkabadi**[2]

Received: 30 July 2023 / Accepted: 27 November 2023

Abstract
Aluminum alloy forms a protective layer of aluminum oxide when exposed to air, which gives it corrosion resistance. But, the layer can be easily damaged, causing metal corrosion. The hard anodizing method is used to solve this issue. Determining the appropriate anodizing parameters, including current density, process time, and electrolyte concentration, is crucial for attaining the desired thickness and hardness of the anodized layer. An experimental design approach utilizing the response surface method (RSM) was employed to investigate the effects of these variables. Quadratic models were presented to predict the hardness and thickness of the layer with an average error of 2.84% and 3.89%, respectively. The models were verified through analysis of variance (ANOVA) to assess the effect of each parameter and their interactions. Oxalic acid concentration, the interaction between process time and oxalic acid concentration, and the square of current density and process time have a significant impact on hardness. Layer thickness is mainly influenced by current density, process time, and the interaction between process time and oxalic acid concentration. Optimization results show that a current density of $1.19 A/dm^2$, a process time of 160 min, sulfuric and oxalic acid concentrations of 26.25 gr/lit and 36.88 gr/lit, respectively, leads to hardness of 434 HV and thickness of 93.6 μm. A scanning electron microscope (SEM) image under optimal conditions shows that aluminum porous arrays created by an anodizing process in mixed sulfuric acid and oxalic acid electrolyte, with a hexagonal shape observed across a wide range of grain domains.

Keywords Anodizing · Hardness · Coating thickness · Response surface method · Optimization

1 Introduction

6000 series of aluminum alloys are popular for structural purposes due to their favorable mechanical properties, including ductility, corrosion resistance, and weldability. Of these alloys, 6063 is particularly resistant to corrosion and anodizing effects. It is commonly used to produce construction parts, kitchen appliances, false ceilings, and extruded architectural components [1]. It forms a thin layer of aluminum oxide (2.5–10 nm) upon exposure to air, which increases its resistance to corrosion. However, this layer can be easily removed and destroyed by chemical and environmental factors, leading to corrosion. Henley et al. found that this protective layer is ineffective in harsh marine environments [2].

One way to decrease corrosion is through the use of protective methods, such as conversion coatings that transform the metal surface into a mineral compound. Examples of these methods include boehmite coating [3], chromate coating [4], phosphate coating [5], and anodizing [6, 7]. Chromate coating, however, is no longer used due to environmental concerns related to chromate compounds. Anodizing is a process that modifies the surface of a metal by oxidizing it with an electrolyte, resulting in a thicker layer. This method increases the hardness and corrosion resistance of aluminum parts, creates a decorative appearance, and modifies some physical properties. Anodizing is used to protect various industrial components against corrosion and to manufacture dielectric films for electrolytic capacitors [6].

Various factors such as the type of electrolyte, temperature, potential, current density, alloy type, and process

✉ Vahid Pouyafar
pouyafar@tabrizu.ac.ir

[1] Department of Manufacturing Engineering, University of Tabriz, Tabriz, Iran

[2] Faculty of Advanced Technologies, University of Mohaghegh Ardabili, Ardabil, Iran

Published online: 27 December 2023

duration affect the anodizing process and the properties of the resulting layer. Therefore, it is crucial to consider these conditions. Research studies have focused on the hardness and wear resistance of aluminum oxide layers resulting from hard anodizing. This method is suitable for applications that require exceptional hardness exceeding 400 Vickers, as its surface hardness surpasses that of various hardened steels and hard chrome plating [8].

Strak et al. determined that the corrosion resistance of the 6063 aluminum alloy is affected by specific mechanical and physical stresses. Temperatures above 60°C significantly impact the anodizing characteristics of the 6063 alloy. Mechanical deformation does not affect the anti-corrosion capabilities of anodized aluminum alloy [9]. Polat et al. [10] used the Taguchi method to optimize the anodic polarization process for 6060 alloy. Four parameters were considered: additive type, dissolved Al concentration, bath temperature, and current densities, organized in an L9 orthogonal array. Anodized samples had various corrosion current densities and potentials, implying modifications in the properties of the anodized layer such as geometry, distribution, and structure. Wilson et al. [11] studied the anodizing of the 6060 aluminum alloy with sulfuric acid to improve corrosion resistance and adhesiveness with the post-painting layer by adding tartaric acid. They also explored the potential of using tartaric-sulfuric acid anodizing (TSA) to enhance the corrosion resistance of the anodic film. Knudsen et al. [12] found that alternating current (AC) hot anodizing is a better pretreatment for organic coating of the 6060 alloy compared to direct current (DC) anodizing. This is due to its ability to clean the surface and improve resistance against corrosion.

The design of experiments (DOE) is a method used to determine the correlation between controllable and response variables in a process. It involves systematically altering relevant factors through experimental plans to identify optimal conditions, significant factors, and the interactions of these factors [13]. The use of DOE is crucial in achieving precise outcomes by optimizing the number of tests. The RSM, which involves statistical experiment design, modeling, and optimization, is a practical approach to experimental design. This method reveals the impact and optimal conditions of primary factors, interactions, nonlinear variables, and the relationship between variables and responses. The central composite design (CCD) method is one of the RSM techniques which uses a second-order model to achieve optimal conditions [14].

To date, there have been limited investigations into utilizing the RSM method to model anodizing experiments for various industrial objectives. The current study focuses on utilizing CCD to implement RSM in order to model and optimize the anodizing experiments of the 6063 aluminum alloy. On the other hand, the center of interest lies in the electrolyte solution employed in this study, which consisted of a mixture of sulfuric and oxalic acids. The study's novelty and objective are to investigate how changing certain parameters, including anodizing time, current intensity, and concentration of electrolyte mixture, would affect the growth of the oxide layer. Using RSM, the researchers aimed to identify the most optimal combination of parameters for anodizing the 6063 aluminum alloy, as previous research on anodizing has yet to establish the ideal parameter set.

2 Materials and Methods

2.1 Sample Preparation

The chemical composition of the 6063 alloy was analyzed using a quantometer, and the results are presented in Table 1. The samples were polished using sandpapers up to 2000 grit, washed in distilled water, degreased with an acetone solution, and then rinsed with distilled water. These processes significantly improved the surface smoothness of the samples.

2.2 Design of experiments

Nowadays, the use of DOE, especially in laboratory and industrial work, has gained interest. It is a fundamental principle for obtaining reliable results, saving time, conducting fewer tests, and optimizing processes. DOE helps to determine optimal values or conditions for compatible responses. Additionally, RSM is a technique for designing experiments with multiple independent variables that affect one or more dependent variables. This method aims to optimize the responses by reducing the number of tests and establishing a mathematical relationship between the variables. RSM is advantageous in determining the optimal or near-optimal responses through a set of tests, making it a popular tool. This study investigated four independent parameters: current density, process time, concentration of sulfuric acid and concentration of oxalic acid, as input parameters and the thickness and hardness of the created layer as output parameters. The experiments were designed using the RSM and the CCD approaches with the help of Design Expert software. Table 2 shows the levels of design factors used in the CCD, which were varied in 5 levels ($-\alpha, -1, 0, +1, +\alpha$). The values for each parameter were chosen based on previous research in the field of anodizing [15–17].

2.3 Anodizing Setup and Required Tests

A specialized anodizing power source made by Silicon Company is used for the oxidation process depicted in Fig. 1a. This power source can provide an output voltage in four different forms (DC, AC, PC, and PRC) and can be adjusted from

Table 1 Chemical composition of 6063 alloy from quantometery

Elements	Al	Si	Mg	Fe	Cu	Cr	Zn	Mn	Ti
Composition (Wt. %)	98.69	0.5	0.45	0.24	0.03	0.03	0.02	0.03	0.01

Table 2 The factors and their levels used in the CCD

Factor	Level				
	− 2 (− α)	− 1	0	1	2 (α)
Current density (A/dm^2)	0.3	0.6	0.9	1.2	1.5
Process time (min)	40	80	120	160	200
Sulfuric acid (g/l)	5	26.25	47.5	68.75	90
Oxalic acid (g/l)	20	35	50	65	80

Fig. 1 Anodizing setup **a** power supply, **b** cooling system and **c** aluminum sample pre- and post-anodizing

zero to 60 V. Studies in the field of using solutions containing different acids have shown that the anodic films formed in the combined solution of oxalic and sulfuric acid have better corrosion resistance compared to using these acids separately [18]. So, to improve the quality of the anodic layer, a mixed solution of sulfuric and oxalic acid was suggested according to Table 2. The sample diameter was measured three times with a micrometer of 0.001 mm resolution before anodizing. In anodic oxidation, a pure lead sheet is connected to the negative pole as the common cathode. Without an electric current, the sheet will gradually dissolve in the electrolyte solution. It is crucial to maintain a minimum cathode-to-anode area ratio of 3 to 1. A cooling system is used during the anodizing process to prevent polarizations and maintain a uniform temperature (Fig. 1b). Compressed air is introduced into the electrolyte solution in a controlled manner to maintain its chemical composition. After the process, the sample is exposed to boiling water for 30 min, and its diameter is measured at three different points. Figure 1c shows the aluminum sample before and after anodizing.

The ASTM E92 standard was followed to determine the hardness of the coating, using an SCTMC microhardness tester [19]. Vickers hardness was used to measure the surface hardness, with a load of 50g for 15 s. Each sample was tested and measured at three different points, with a tolerance of ± 5 HV. The microstructure of the samples was examined using an SEM (MIRA3 FEG-SEM) from Czech Republic.

3 Results and Discussion

3.1 Experiment Results

Table 3 displays the results of 30 experiments designed using Design Expert 11 software. To determine the required number of experiments for the anodizing process with the RSM

Table 3 Experimental design and results of the CCD

Std	Run	Processing parameters				Response	
		Density (A/dm^2)	Time (min)	Sulfuric acid (g/l)	Oxalic acid (g/l)	Hardness (HV)	Thickness (μm)
7	1	0.6	160	68.75	35	455	26
9	2	0.6	80	26.25	65	342	23
17	3	0.3	120	47.5	50	367	6
20	4	0.9	200	47.5	50	361	94
5	5	0.6	80	68.75	35	416	20
14	6	1.2	80	68.75	65	437	59
15	7	0.6	160	68.75	65	397	64
22	8	0.9	120	90	50	470	63
16	9	1.2	160	68.75	65	333	103
18	10	1.5	120	47.5	50	371	89
24	11	0.9	120	47.5	80	371	71
25	12	0.9	120	47.5	50	453	59
29	13	0.9	120	47.5	50	422	65
12	14	1.2	160	26.25	65	341	110
28	15	0.9	120	47.5	50	430	59
23	16	0.9	120	47.5	20	416	52
6	17	1.2	80	68.75	35	408	76
3	18	0.6	160	26.25	35	409	52
1	19	0.6	80	26.25	35	344	32
13	20	0.6	80	68.75	65	456	14
8	21	1.2	160	68.75	35	417	90
26	22	0.9	120	47.5	50	413	61
4	23	1.2	160	26.25	35	435	92
11	24	0.6	160	26.25	65	299	90
10	25	1.2	80	26.25	65	410	45
27	26	0.9	120	47.5	50	459	63
21	27	0.9	120	5	50	441	90
2	28	1.2	80	26.25	35	342	68
19	29	0.9	40	47.5	50	353	27
30	30	0.9	120	47.5	50	440	64

and CCD, the formula $N = 2^k + 2K + C_p$ is utilized, where k represents the number of factors and C_p represents the number of repetitions of the central point. The values of these factors are 4 and 6, respectively.

3.2 Regression Models and Analysis of Variance

RSM involves statistical methods and appropriate DOE to determine the interaction among process variables, making it different from conventional methods. Two main designs for RSM are CCD and Box–Behnken design (BBD). CCD can fit a quadratic model and is suitable for sequential experimentation, incorporating information from a factorial experiment. BBD needs fewer design points than CCD, making it less expensive while maintaining the same number of factors. BBD always has three levels per factor; while, CCD can have up to five. Rashid et al. [20] studied the corrosion tendency of 6061 aluminum alloy during anodizing with chromic acid. They used a CCD method to reduce the required tests to 28, while still analyzing four parameters with five levels. Nualsing et al. [21] optimized anodizing parameters to enhance aluminum oxide film production on aluminum foil using the BBD approach for experimental design and statistical analysis.

The RSM method commonly employs a quadratic equation, presented in Eq. 1, to describe the response behavior.

$$Y = \beta_0 + \sum_{i=1}^{n} \beta_i X_i + \sum_{i=1}^{n} \beta_{ii} X_i^2 + \sum_{i \neq 1 j=1}^{n} \beta_{ij} X_i X_j + \varepsilon \quad (1)$$

The given equation represents the predicted response Y as a function of independent variables X_i and X_j, along with individual, quadratic, and interaction term coefficients β_i, β_{ii}, and $\beta_{ij,}$, respectively. The constant coefficient is represented by β_0. The number of independent variables is denoted by n, and the error term is represented by $\mathfrak{E}$ [22].

ANOVA can assess the validity of an equation or model by identifying significant and insignificant parameters, determining the effectiveness of investigated factors on the output, and calculating quadratic or second-order model coefficients. It uses a signal-to-noise ratio to measure the impact of uncontrollable factors on a qualitative characteristic in a controlled process. A higher signal-to-noise ratio indicates better sensitivity to controllable parameters. The total signal-to-noise value for each output is calculated using Eq. 2.

$$\eta = -10\log\left[\frac{1}{P}\sum_{i=1}^{P}\frac{1}{w_i^2}\right] \quad (2)$$

where η, P, and w_i represent the signal-to-noise ratio, the number of repetitions, and the measured output in each experiment. Equations 3, 4, 5 and 6 are utilized to compute the parameters associated with variance analysis, including the total sum of square deviation (SST), total degree of freedom (f_T), the sum of square deviation of jth factor (SS_j) and its degree of freedom (f_j) [22].

$$SST = \sum_{i=1}^{n} \eta_i^2 - \frac{T^2}{n} \quad (3)$$

$$f_T = n - 1 \quad (4)$$

$$SS_j = \frac{1}{r}\sum_{i=1}^{m} T_i^2 - \frac{T^2}{n} (j = 1, 2, \ldots, k) \quad (5)$$

$$f_j = m - 1 \quad (6)$$

where n is the total number of experiments, m is the number of levels for each factor, k is the number of columns of the orthogonal array, $r = n/m$, T is the total sum of S/N ratio, and Ti is the sum of S/N ratio when the level of factors is fixed on the ith row for an arbitrary column.

The sum of square of error (SSE) and its degree of freedom (f_e), the variance of jth parameter (MS_j) and the variance of error (MSE) can be calculated as follows [22]:

$$SSE = SST - \sum_{j=1}^{k} SS_j \quad (7)$$

$$f_e = f_T - \sum_{j=1}^{k} f_j \quad (8)$$

$$MS_j = \frac{SS_j}{f_i} \quad (9)$$

$$MSE = \frac{SSE}{f_e} \quad (10)$$

Equation 11 provides the F-value for the jth factor.

$$F_j = \frac{MS_j}{MSE} \quad (11)$$

Equation 12 can be used to calculate the contribution percentage (Pc) of each parameter on the results.

$$P_c(\%) = \frac{SS_j - f_j.MSE}{SST} \times 100 \quad (12)$$

The resulting measurements of anodized layer hardness and thickness are presented in Table 4. The quadratic models were found to have an average error of 2.84% and 3.89% in predicting the hardness and thickness of the layer, respectively.

The quadratic model was the most appropriate for both output variables and was selected for further analysis. Table 5 shows the findings.

Tables 6 and 7 show the results of the ANOVA analysis for hardness and thickness responses. The key parameters for evaluating the model, the parameters, and their interactions include *p*-value and *F*-value. *F*-value indicates data distribution, with higher values being more desirable for each input variable. The *p*-value reflects the significance of each term in the response, with values less than 0.05 indicating significance for each variable. If any variable has a *p*-value greater than 0.1, it is deemed insignificant. This analysis is critical for determining response validity.

According to Table 6, the *p*-values for sulfuric acid concentration (C), oxalic acid concentration (D), interaction of current density and sulfuric acid concentration (AC), interaction of process time and sulfuric acid concentration (BC), interaction of process time and oxalic acid concentration (BD), and the second power of current density, the process time, and the concentration of oxalic acid (A^2, B^2, D^2) are less than 0.05. This indicates their significant contribution to the hardness of the samples.

According to Table 7, the thickness of the coating is significantly influenced by several factors, such as current density

Table 4 Comparison between the experimental and predicted results of anodized layer's hardness and thickness by the CCD

Std	Run	Processing parameters				Response 1, Hardness (HV)			Response 2, Thickness (μm)		
		A	B	C	D	Experimental	Predicted	Error (%)	Experimental	Predicted	Error (%)
7	1	0.6	160	68.75	35	455	450	1.09	26	25.9	0.16
9	2	0.6	80	26.25	65	342	367	6.92	23	27.1	15.21
17	3	0.3	120	47.5	50	367	372	1.32	6	5.6	7.46
20	4	0.9	200	47.5	50	361	355	1.64	94	96.3	2.42
5	5	0.6	80	68.75	35	416	422	1.52	20	18.6	7.38
14	6	1.2	80	68.75	65	437	425	2.73	59	57.3	2.98
15	7	0.6	160	68.75	65	397	376	5.46	64	62.5	2.47
22	8	0.9	120	90	50	470	471	0.12	63	65.7	4.18
16	9	1.2	160	68.75	65	333	337	1.16	103	105.1	2.02
18	10	1.5	120	47.5	50	371	370	0.25	89	86.9	2.40
24	11	0.9	120	47.5	80	371	373	0.46	71	68.5	3.65
25	12	0.9	120	47.5	50	453	442	2.47	59	61.0	3.28
29	13	0.9	120	47.5	50	422	442	4.54	65	61.0	6.56
12	14	1.2	160	26.25	65	341	356	4.19	110	111.6	1.46
28	15	0.9	120	47.5	50	430	442	2.73	59	61.0	3.28
23	16	0.9	120	47.5	20	416	418	0.43	52	53.5	2.80
6	17	1.2	80	68.75	35	408	392	4.06	76	78.8	3.54
3	18	0.6	160	26.25	35	409	409	0.07	52	53.9	3.63
1	19	0.6	80	26.25	35	344	320	7.36	32	31.1	2.81
13	20	0.6	80	68.75	65	456	452	0.99	14	14.6	4.27
8	21	1.2	160	68.75	35	417	424	1.59	90	86.1	4.50
26	22	0.9	120	47.5	50	413	442	6.58	61	61.0	0.00
4	23	1.2	160	26.25	35	435	436	0.25	92	92.6	0.67
11	24	0.6	160	26.25	65	299	313	4.55	90	90.5	0.51
10	25	1.2	80	26.25	65	410	400	2.53	45	48.3	6.82
27	26	0.9	120	47.5	50	459	442	3.83	63	61.0	3.28
21	27	0.9	120	5	50	441	409	7.74	90	84.7	6.19
2	28	1.2	80	26.25	35	342	362	5.41	68	69.8	2.57
19	29	0.9	40	47.5	50	353	363	2.78	27	25.7	5.19
30	30	0.9	120	47.5	50	440	442	0.47	64	61.0	4.92

Table 5 Model summary statistics for hardness and thickness of layer

Source	Std. Dev	R^2	Adjusted R^2	Predicted R^2	Press	
Hardness						
Linear	2.0E + 07	0.19	0.07	− 0.17	1.5E + 16	
2FI	1.8E + 07	0.53	0.28	0.14	1.1E + 16	
Quadratic	8.4E + 06	0.91	0.84	0.70	3.9E + 15	Suggested
Cubic	9.2E + 06	0.95	0.81	0.08	1.2E + 16	Aliased
Thickness						
Linear	12.1	0.8334	0.81	0.74	5694	
2FI	7.3	0.9542	0.93	0.92	1839	
Quadratic	3.2	0.9929	0.98	0.97	750	Suggested
Cubic	2.5	0.9979	0.99	0.92	1823	Aliased

Table 6 ANOVA for response surface quadratic model for hardness

Source	Sum of squares	df	Mean square	*F*-value	*p*-value	
Model	1.2E + 16	14	8.6E + 14	12.04	< 0.0001	significant
A-Density	8.3E + 11	1	8.3E + 11	0.01	0.9154	
B-Time	1.4E + 13	1	1.4E + 13	0.19	0.6635	
C-Sulfuric Acid	1.9E + 15	1	1.9E + 15	26.65	0.0001	
D-Oxalic acid	6.7E + 14	1	6.7E + 14	9.38	0.0079	
AB	6.9E + 13	1	6.9E + 13	0.96	0.3405	
AC	8.6E + 14	1	8.6E + 14	12.14	0.0033	
AD	1.8E + 13	1	1.8E + 13	0.26	0.6143	
BC	3.9E + 14	1	3.9E + 14	5.52	0.0329	
BD	2.9E + 15	1	2.9E + 15	41.63	< 0.0001	
CD	4.6E + 13	1	4.6E + 13	0.65	0.4322	
A^2	1.9E + 15	1	1.9E + 15	27.40	0.0001	
B^2	2.5E + 15	1	2.5E + 15	35.61	< 0.0001	
C^2	1.9E + 14	1	1.9E + 14	2.77	0.1165	
D^2	8.6E + 14	1	8.6E + 14	12.16	0.0033	
Residual	1.0E + 15	15	7.1E + 13			
Lack of Fit	5.4E + 14	10	5.4E + 13	0.52	0.8192	not significant
Pure Error	5.2E + 14	5	1.0E + 14			
Cor Total	1.3E + 16	29				

Table 7 ANOVA for response surface quadratic model for layer thickness

Source	Sum of squares	df	Mean square	*F*-value	*p*-value	
Model	21,793	14	1556	150	< 0.0001	significant
A-Density	9922	1	9922	961	< 0.0001	
B-Time	7490	1	7490	725	< 0.0001	
C-Sulfuric Acid	541	1	541	52	< 0.0001	
D-Oxalic acid	337	1	337	32	< 0.0001	
AB	1	1	1	0.09	0.7599	
AC	462	1	462	44	< 0.0001	
AD	306	1	306	29	< 0.0001	
BC	240	1	240	23	0.0002	
BD	1640	1	1640	158	< 0.0001	
CD	1	1	1	0.09	0.7599	
A^2	394	1	394	38	< 0.0001	
B^2	8	1	8	0.77	0.3912	
C^2	328	1	328	31	< 0.0001	
D^2	2	1	2	0.22	0.6413	
Residual	154	15	10			
Lack of Fit	122	10	12	1.86	0.2562	not significant
Pure Error	32	5	6			
Cor Total	21,948	29				

Table 8 ANOVA for response surface reduced quadratic model for hardness

Source	Sum of squares	df	Mean square	*F*-value	*p*-value	
Model	1.1E + 16	11	1.0E + 15	16	< 0.0001	significant
A-Density	8.3E + 11	1	8.3E + 11	0.01	0.9125	
B-Time	1.4E + 13	1	1.4E + 13	0.20	0.6523	
C-Sulfuric Acid	1.9E + 15	1	1.9E + 15	28	< 0.0001	
D-Oxalic acid	6.7E + 14	1	6.7E + 14	10	0.0054	
AC	8.6E + 14	1	8.6E + 14	12	0.0021	
BC	3.9E + 14	1	3.9E + 14	5	0.0260	
BD	2.9E + 15	1	2.9E + 15	44	< 0.0001	
A^2	1.9E + 15	1	1.9E + 15	29	< 0.0001	
B^2	2.5E + 15	1	2.5E + 15	38	< 0.0001	
C^2	1.9E + 14	1	1.9E + 14	3	0.1026	
D^2	8.6E + 14	1	8.6E + 14	13	0.0020	
Residual	1.2E + 15	18	6.7E + 13			
Lack of Fit	6.8E + 14	13	5.2E + 13	0.5034	0.8522	not significant
Pure Error	5.2E + 14	5	1.0E + 14			
Cor Total	1.3E + 16	29				
Std. Dev	8.1E + 06		R^2	0.9080		
Mean	6.6E + 07		Adjusted R^2	0.8518		
C.V. %	12.31		Predicted R^2	0.7583		
			Adeq Precision	15.5254		

(A), process time (B), concentration of sulfuric acid (C), concentration of oxalic acid (D), interaction of current density and concentration of sulfuric acid (AC), interaction of current density and concentration of oxalic acid (AD), interaction of process time and concentration of sulfuric acid (BC), interaction of process time and concentration of oxalic acid (BD), and the square power of the current density and concentration of sulfuric acid (V). These factors have a substantial impact on the coating thickness as their p value is less than 0.05.

The significance of a model is determined by the lack of fit value obtained from repeating the central point. Tables 6 and 7 show that both outputs have an insignificant value, which confirms the validity of the model and the accuracy of the data. To enhance the model's accuracy, any factors with a p value exceeding 0.1 are eliminated. The remaining parameters undergo a new variance analysis, with the results exhibited in Tables 8 and 9.

Table 8 shows that the model has a significant F-value of 16.15 with a very low probability of occurrence. Significant model terms include C, D, AC, BC, BD, A^2, B^2, and D^2, while reducing insignificant terms may be beneficial. The Lack of Fit F-value is 0.50, indicating that it is insignificant compared to pure error, which is desirable for a good model fit.

Table 9 shows that the model has a significant F-value of 249.07, indicating that the chance of such a considerable value occurring due to noise is only 0.01%. Model terms with *P*-values less than 0.05, including A, B, C, D, AC, AD, BC, BD, A^2, and C^2, are also significant. However, model terms with values greater than 0.1 are insignificant. A Lack of Fit *F*-value of 1.45 suggests that the Lack of Fit is not significant compared to pure error. There is a 36.05% chance that this Lack of Fit *F*-value is due to noise. A Lack of Fit that is not significant is desirable as it indicates a well-fitting model.

Tables 8 and 9 show the statistical parameters for the models. The R-square value indicates the degree of overlap between laboratory data and predicted values. In the hardness model, the R^2 value suggests that 90% of the available variation is described. The adjusted R^2 is 0.85, which is a more accurate measure of the model's usefulness. The agreement between $R^2_{\text{Adj}} = 0.85$ and $R^2_{\text{Pred}} = 0.75$ is reasonable. The Adeq. precision ratio is 15.5254, indicating a satisfactory signal to noise ratio. The low coefficient of variation (C.V.) value of 12.31% shows greater precision and reliability of testing outcomes.

The model for the thickness of the anodized layer has an R^2 value of 99%, which means that the model can explain 99% of the variations. The adjusted R^2 of 0.98 agrees with the predicted R^2 of 0.97. The Adeq. precision ratio is 59.2169, indicating that the model can be used for design space navigation. The low C.V. value of 4.86% indicates improved precision and reliability of test results. Equation 13 uses reduced quadratic regression with an inverse square root power function ($\lambda = 3$, $k = 0$) to transform Y and describes

Table 9 ANOVA for response surface reduced quadratic model for thickness

Source	Sum of squares	df	Mean square	*F*-value	*p*-value	
Model	21,782	10	2178	249	< 0.0001	significant
A-Density	9922	1	9922	1134	< 0.0001	
B-Time	7490	1	7490	856	< 0.0001	
C-Sulfuric Acid	541	1	541	61	< 0.0001	
D-Oxalic acid	337	1	337	38	< 0.0001	
AC	462	1	462	52	< 0.0001	
AD	306	1	306	35	< 0.0001	
BC	240	1	240	27	< 0.0001	
BD	1640	1	1640	187	< 0.0001	
A^2	386	1	386	44	< 0.0001	
C^2	361	1	361	41	< 0.0001	
Residual	166	19	8			
Lack of Fit	133	14	9	1.45	0.3605	not significant
Pure Error	32	5	6			
Cor Total	21,948	29				
Std. Dev	2.96		R^2	0.9924		
Mean	60.90		Adjusted R^2	0.9884		
C.V. %	4.86		Predicted R^2	0.9760		
			Adeq Precision	59.2169		

the relationship between hardness and test variables. Equation 14, expressed in actual factors, was derived using the values obtained from the CCD for layer thickness.

$$\begin{aligned}(\text{Hardness})^3 = &-3.46949\text{E}+08+2.23208\text{E}+08(\text{A})\\&+2.83922\text{E}+06(\text{B})+1.59410\text{E}+06(\text{C})\\&+4.87597\text{E}+06(\text{D})-1.15488\text{E}+06(\text{AC})\\&-5842.46640(\text{BC})-22722.54573(\text{BD})\\&-9.38735\text{E}+07\left(\text{A}^2\right)-6019.66646\left(\text{B}^2\right)\\&+5952.81170\left(\text{C}^2\right)-25015.82319\left(\text{D}^2\right)\end{aligned} \tag{13}$$

$$\begin{aligned}\text{Thickness} = &-2.71086++150.08987(\text{A})-0.185539(\text{B})\\&-1.18478(\text{C})-0.9(\text{D})+0.843137(\text{AC})\\&-0.972222(\text{AD})-0.004559(\text{BC})\\&+0.016875(\text{BD})\ -40.97222(\text{A2})\\&+0.007889(\text{C2})\end{aligned} \tag{14}$$

The normal distribution of errors is a common assumption in statistics, and to verify this assumption in test data, the normal plot of residuals is employed. If the error distribution shows a linear pattern and is not S-shaped, then it can be concluded that the errors follow a normal distribution. The graphs shown in Figs. 2a and 3a illustrate that the experimental data closely match a linear distribution, suggesting that the models accurately reflect a normal distribution.

The plots in Figs. 2b and 3b display the externally studentized residuals versus the run number for the hardness and thickness of the layer. The data appears to be randomly scattered, indicating the absence of any hidden variability during the experiment.

To verify the accuracy of the results, an analysis was conducted on the data to determine the correlation between the predicted values derived from the quadratic equation and the actual response data obtained from the experiments designed by the CCD model. This analysis is illustrated in Figs. 2c and 3c. The data points on the plot were close to the straight line, which indicates a strong correlation between the experimental and predicted values. This implies that the assumptions made during the analysis were valid and reliable.

3.3 Analysis of the Effect of Variable Parameters Using 2D and 3D Response Surface Plots

Figure 4 shows the response surfaces in 2D and 3D forms, illustrating the interaction of parameters affecting coating hardness. The interaction effect between two parameters has been analyzed by assuming that the value of the remaining parameters is constant and equal to the central point of their respective levels. The results indicate that changes in current density have a more significant impact on coating hardness

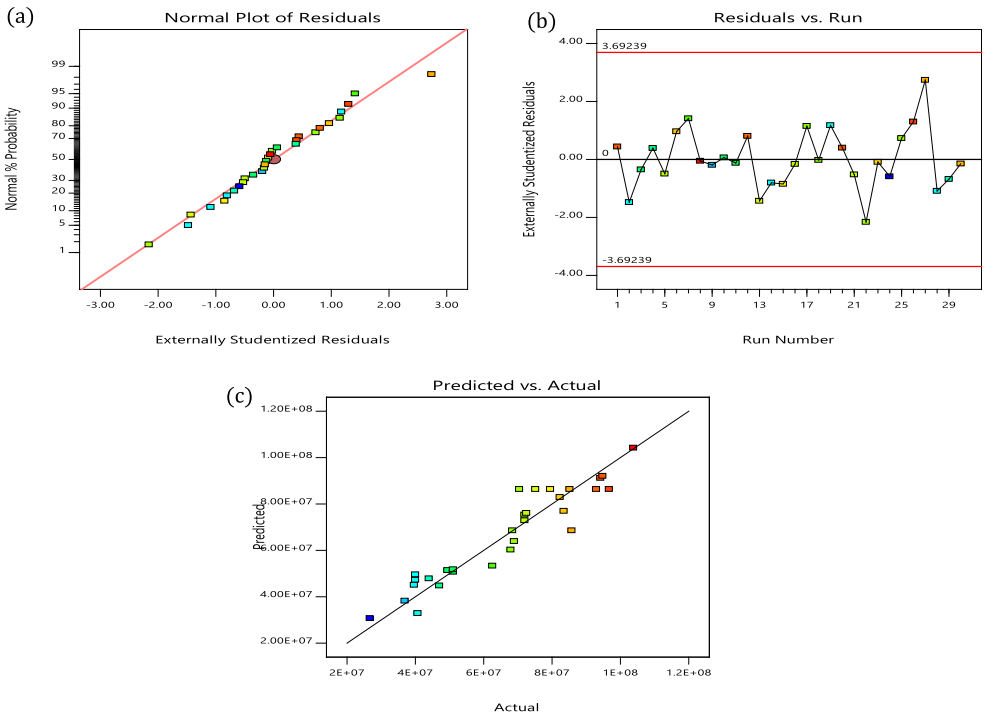

Fig. 2 **a** Normal plot of residuals, **b** residuals vs. run number and **c** predicted vs. actual values for hardness

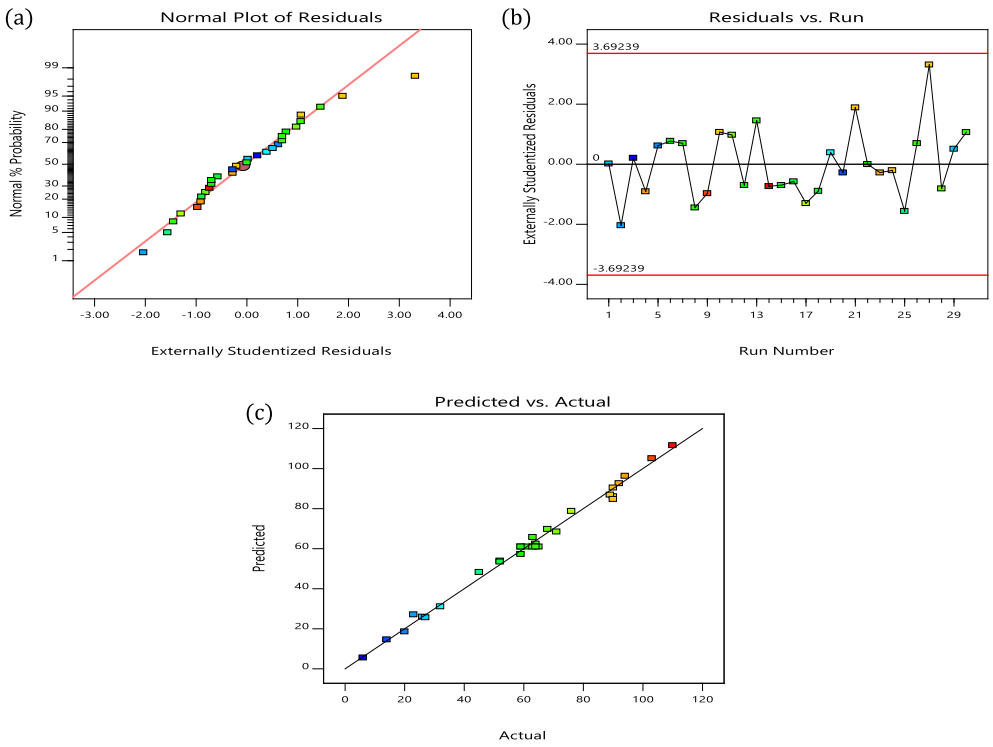

Fig. 3 **a** Normal plot of residuals, **b** residuals vs. run number and **c** predicted vs. actual values for thickness

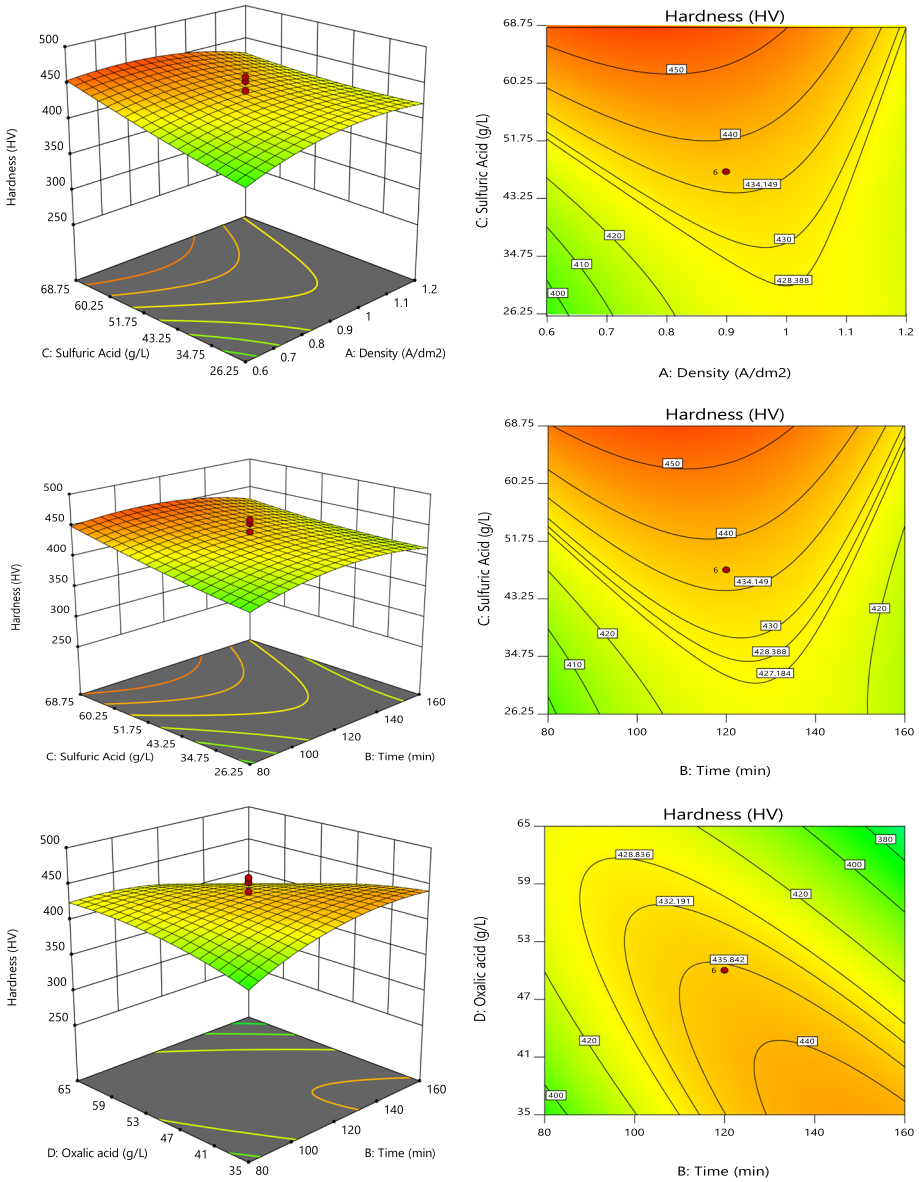

Fig. 4 2D and 3D response surface plots of the interaction between parameters for the hardness response

than sulfuric acid concentration. Increasing sulfuric acid concentration slightly increases coating hardness. However, the highest hardness value was observed with the highest sulfuric acid concentration and average current density. When analyzing the combined effect of process time and sulfuric acid concentration while keeping the other parameters constant, it becomes apparent that changes in process time have a minimal influence on the hardness of the coating. Nevertheless, increased sulfuric acid concentration leads to a rise in coating hardness. Upon analyzing the interaction effect of process time and oxalic acid concentration, it was noticed that augmenting the process time at lower oxalic acid concentrations resulted in a slight enhancement in hardness.

Increasing current density and anodizing time increases the voltage required to create the anodic layer, resulting in a decrease in porosity and smaller cell size. This leads to an increased hardness of the anodic oxide layer. During anodizing, two types of dissolution occur: chemical and electric field-assisted. Chemical dissolution is influenced by the concentration of the electrolyte and operation time; while, field-assisted dissolution is caused by increased electrical current and thermal heating. To achieve high coating hardness, higher current density, longer process time, and higher concentration of sulfuric acid are needed. Increasing the concentration of oxalic acid improves the growth rate of the anodic oxide layer, reduces porosity, and slightly increases the hardness.

Figure 5 illustrates the response surfaces for the interaction of effective parameters on thickness response in both 2D and 3D. The coating thickness increases with an increase in

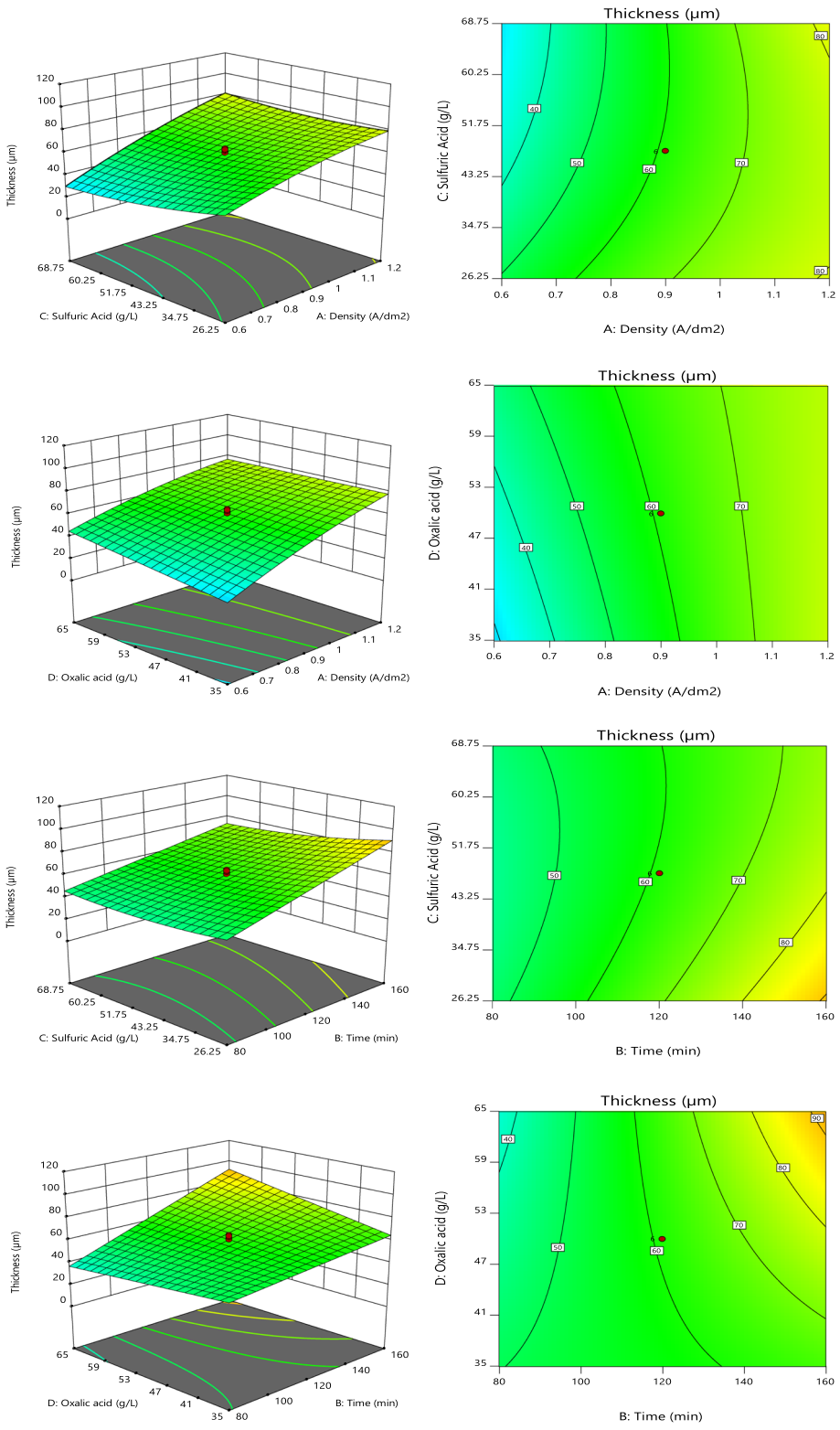

Fig. 5 2D and 3D response surface plots of the interaction between parameters for the thickness response

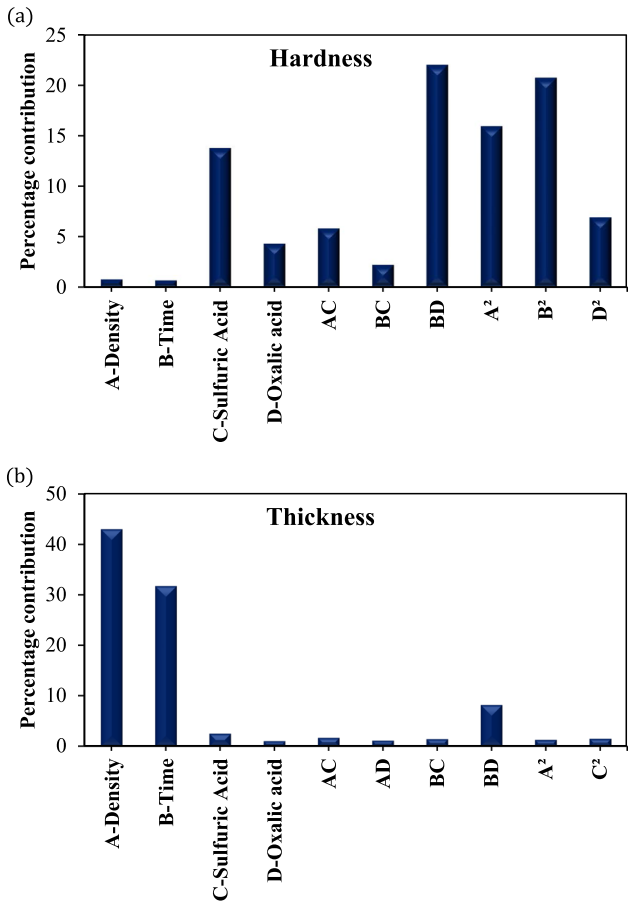

Fig. 6 Percentage contribution of effective parameters and their interactions on **a** hardness and **b** thickness of the layer

current density and process time. The effect of current density on thickness is more significant than that of anodizing time. To obtain a uniform, non-porous aluminum oxide layer, extending the anodizing time is advantageous. The figure also shows that the thickness of the coating increases with high current density and oxalic acid concentration. A thicker anodic layer is produced at a high current density, whereas a thinner layer is formed with low current density and oxalic acid concentration.

When the current density is higher, a greater voltage is required for the anodic layer to form, resulting in a decrease in the porosity of the oxide coating due to fewer forming cells. As a result, the anodic layer becomes thicker. The thickness of the anodic layer increases due to several factors, such as the concentration of oxalic acid, which increases the resistance of the electrochemical cell. The thickness is also affected by the concentration of sulfuric acid and current density, where higher values result in thicker layers.

Using Tables 6 and 7, we analyzed the effect of input variables on hardness and thickness through Eq. 12. The results in Fig. 6 show that the concentration of sulfuric acid, the interaction between process time and oxalic acid, and the square of current density and time have the most significant impact on hardness. In contrast, layer thickness is mainly influenced by current density, process time, and the interaction between process time and oxalic acid.

3.4 Optimization

Once the factors that impact the system's performance have been identified, the next step is to modify them to determine the optimal conditions for the best possible outcome. The anodizing process's conditions must be optimized, which involves determining the range of input parameters such as current density, process time, and concentration of sulfuric and oxalic acid. This research aims to maximize the hardness and thickness of the resulting layer. Design Expert software provides 80 solutions for optimizing the anodizing process's conditions, with the first one chosen as the optimal condition (Table 10). The results indicate that this selection has a desirability of 0.81, meaning that if the anodizing process is conducted with a current density of $1.19 A/dm^2$, a process duration of 160 min, and sulfuric and oxalic acid concentrations of $26.25 gr/lit$ and $36.88 gr/lit$, respectively, there is an 81% chance of achieving a hardness of 434 HV and a thickness of 93.6 μm.

Experiments were conducted three times under optimal conditions. Table 10 presents the average values for hardness and coating thickness, which are in line with the software's predictions, indicating high model accuracy. Figure 7 shows a schematic representation of the determined optimal points.

3.5 Microstructure Investigation

The SEM images presented in Fig. 8 depict the polished and anodized layer that has formed on the sample's surface under optimal conditions. A polished sample image in Fig. 8a is provided for the purpose of comparison and to display the final outcome. The anodizing process has successfully created aluminum porous arrays in the mixed electrolytes of sulfuric acid and oxalic acid. When alloy 6063 is subjected to anodizing, a thin, porous oxide layer is formed on its surface through a process involving the application of direct current. This layer serves as a base for further growth and allows the electrolyte to penetrate deeper layers. Oxygen evolution takes place at the alloy surface due to the applied current, which reacts with the metal ions from the alloy and results in the growth of metal oxide compounds. The anodizing process continues until the oxide layer reaches the desired thickness. Overall, anodizing provides a controlled and uniform formation of metal oxides on the surface of alloy 6063, resulting in improved corrosion resistance and aesthetic appearance. The hexagonal shape of the arrays can be observed across a wide range of grain domains. By adjusting anodizing conditions such as temperature, applied voltage, operation time,

Table 10 Optimized anodizing process values and comparison with predicted experimental results

Density	Time	Sulfuric acid	Oxalic acid	Desirability	Hardness (HV)			Thickness (μm)		
					Error (%)	Pred.	Exp.	Error (%)	Pred.	Exp.
1.193	160	26.250	36.889	0.816	0.52	434	432	3.9	93.6	90

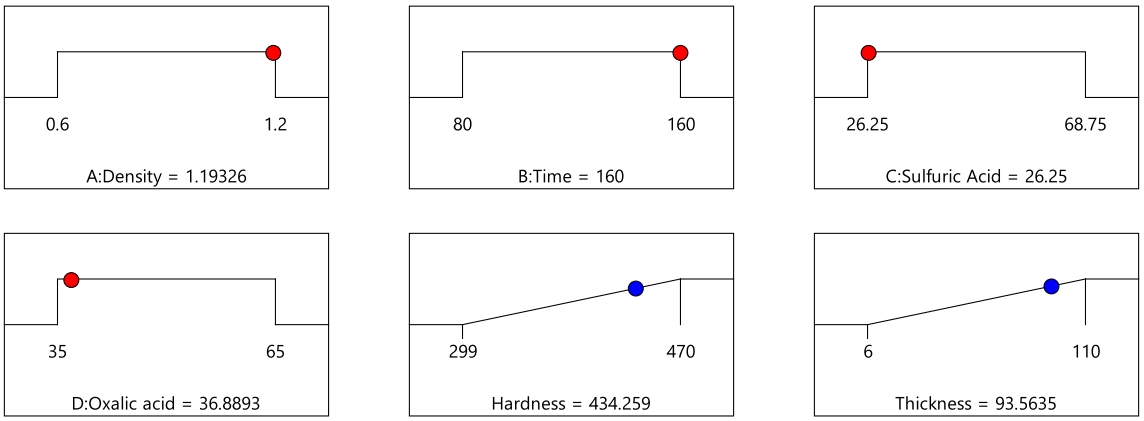

Fig. 7 Optimum parameters of anodizing process

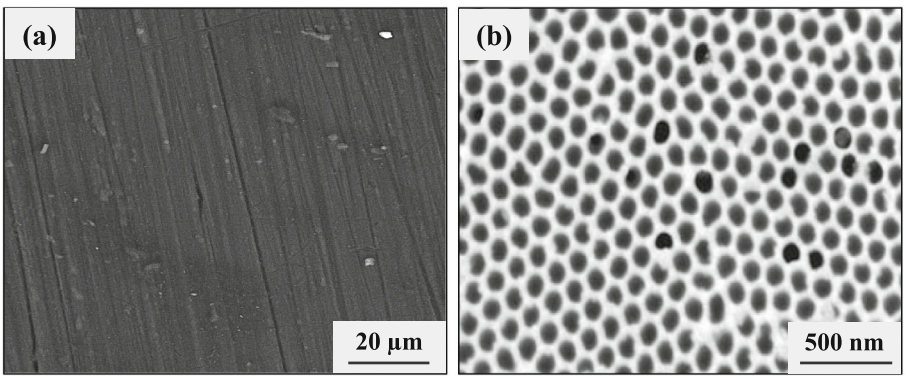

Fig. 8 SEM images of the 6063 alloy **a** polished surface (MAG: 1.5kX) and **b** anodized surface in optimal conditions (MAG: 50kX)

and electrolyte, the diameter of the holes can be controlled. The black dots in Fig. 8b indicate the created holes, which have a diameter of 45 nm under optimal conditions.

4 Conclusions

This study investigated the effects of current intensity, process time, and sulfuric acid and oxalic acid concentrations on the thickness and hardness of the anodic layer produced on 6063 aluminum alloy through anodizing. DOE and RSM methods were used to validate the experimental results and reduce the number of required experiments. Quadratic models with an average error of 2.84% and 3.89% were presented to predict the thickness and hardness of the layer, respectively. ANOVA was utilized to determine the significant parameters and their interactions. The analysis of statistical parameters confirmed the accuracy and reliability of the models in predicting results. Results indicate that the concentration of sulfuric acid, the interaction between process time and oxalic acid, and the square of current density and process time have the most significant impact on hardness. On the other hand, layer thickness is mainly influenced by current density, process time, and the interaction between process time and oxalic acid concentration. The optimum parameters were a current density of $1.19 A/dm^2$, a process time of 160 min, and sulfuric and oxalic acid concentrations of $26.25 gr/lit$ and $36.88 gr/lit$, respectively, with an 81% chance of achieving a hardness of 434 HV and a thickness of 93.6 μm. An SEM image showed aluminum porous arrays created by an anodizing process in a mixed sulfuric acid and oxalic acid electrolyte, with a hexagonal shape observed across a wide range of grain domains.

References

1. Georgantzia, E.; Gkantou, M.; Kamaris, G.S.: Aluminium alloys as structural material: a review of research. Eng. Struct. **227**, 111372 (2021)
2. Henley, V., (2013) Anodic oxidation of aluminium and its alloys: the pergamon materials engineering practice series: Elsevier
3. Kimura, F.; Yamaguchi, E.; Horie, N.; Suzuki, G.; Kajihara, Y.: Formation of boehmite crystals on microblasted aluminum surface to enhance performance of metal–polymer direct joining. Mater. Lett. **260**, 126963 (2020)
4. Becker, M.: Chromate-free chemical conversion coatings for aluminum alloys. Corros. Rev. **37**, 321–342 (2019)
5. Zeng, R.-C.; Zhang, F.; Lan, Z.-D.; Cui, H.-Z.; Han, E.-H.: Corrosion resistance of calcium-modified zinc phosphate conversion coatings on magnesium–aluminium alloys. Corros. Sci. **88**, 452–459 (2014)
6. Araujo, J.V.D.S.; Milagre, M.; Costa, I.: A historical, statistical and electrochemical approach on the effect of microstructure in the anodizing of Al alloys: a review. Crit. Rev. Solid State Mater. Sci. (2023). https://doi.org/10.1080/10408436.2023.2230250
7. Hassanzadeh, N.; Omidvar, H.; Poorbafrani, M.; Tabaian, S.H.: Influence of anodizing parameters on pore diameter of anodic aluminium oxide (aao) films using taguchi design. Arab. J. Sci. Eng. **38**, 1305–1312 (2013)
8. Miramontes, J.C.; Gaona, T.C.; García, M.E.; Esneider Alcála, M.Á.; Maldonado-Bandala, E.; Lara-Banda, M.; Nieves-Mendoza, D.; Olguín-Coca, J.; Zambrano-Robledo, P.; López-León, L.D.: Corrosion resistance of aluminum alloy AA2024 with hard anodizing in sulfuric acid-free solution. Materials. **15**, 6401 (2022)
9. Strąk, A.; Małek, M.; Chlanda, A.; Sudoł, E.: The impact of temperature and mechanical load on corrosion resistance of anodized aluminum EN AW-6063 (T6 temper) alloy for potential architectonic application. J. Build. Eng. **50**, 104128 (2022)
10. Polat, B.D.; Bilici B.; Afşin P.; Akyil C.; Keles O. *A Study of Taguchi Method to Optimize 6XXX Series Aluminium Anodic Oxide Film's Hardness and Investigation of Corrosion Behaviors of Oxide Films*. in *TMS 2016 145th Annual Meeting & Exhibition*. 2016. Cham: Springer International Publishing.
11. Avelar-Batista Wilson, J.C.; Grabowski, A.; Kustosik, K.; Wilson, A.D.: Tartaric acid cross-contamination in post-cascade rinses after sulphuric acid anodising (SAA): effect on adhesive bond strength of AA6060-T6 alloy. Int. J. Adhes. Adhes. **81**, 30–35 (2018)
12. Knudsen, O.Ø.; Tanem, B.S.; Bjørgum, A.; Mårdalen, J.; Hallenstvet, M.: Anodising as pre-treatment before organic coating of extruded and cast aluminium alloys. Corros. Sci. **46**, 2081–2095 (2004)
13. Antony, J., (2023) *Design of experiments for engineers and scientists*: Elsevier
14. Chen, W.-H.; Uribe, M.C.; Kwon, E.E.; Lin, K.-Y.A.; Park, Y.-K.; Ding, L.; Saw, L.H.: A comprehensive review of thermoelectric generation optimization by statistical approach: Taguchi method, analysis of variance (ANOVA), and response surface methodology (RSM). Renew. Sustain. Energy Rev. **169**, 112917 (2022)
15. Abdel-Salam, O.E.; Shoeib, M.A.; Elkilany, H.A.: Characterization of the hard anodizing layers formed on 2014–T3 Al alloy, in sulphuric acid electrolyte containing sodium lignin sulphonate. Egypt. J. Pet. **27**, 497–504 (2018)
16. Sieber, M.; Morgenstern, R.; Scharf, I.; Lampke, T.: Effect of nitric and oxalic acid addition on hard anodizing of AlCu4Mg1 in sulphuric acid. Metals. **8**, 139 (2018)
17. Adyono, N.; Surojo E.; Triyono: Hard anodizing of 6061-T0 aluminium alloy in sulfuric acid bath at low temperature and its micro-hardness properties. AIP Conference Proceedings. 2097, (2019)
18. Rashid, K.H.; Khadom, A.A.: Sulfosalicylic/oxalic acid anodizing process of 5854 aluminum-magnesium alloy: Influence of sealing time and corrosion tendency. Results Chem. **4**, 100289 (2022)
19. Vander Voort, G.F., *Metallography, principles and practice*1999: ASM international.
20. Rashid, K.H.; Khadom, A.A.; Mahood, H.B.: Aluminum ASA 6061 anodizing process by chromic acid using Box-Wilson central composite design: optimization and corrosion tendency. Met. Mater. Int. **27**, 4059–4073 (2021)
21. Nualsing, D.; Pannucharoenwong, N.; Rattanadecho, P.; Echaroj, S.; Benjapiyaporn, C.; Benjapiyaporn, J.: Textural characteristic of anodized aluminium foil for thermal energy storage application. Energy Rep. **7**, 720–729 (2021)
22. Moradi, M.; Hashemi R.; Kasaeian-Naeini M.: Experimental investigation of parameters in fused filament fabrication 3D printing process of ABS plus using response surface methodology. The International Journal of Advanced Manufacturing Technology. 1–18 (2023)